

## Local structure around Ga in ultrafine GaN/ZnO coaxial nanorod heterostructures

S.-W. Han<sup>a)</sup> and H.-J. Yoo

*Institute of Proton Accelerator, Institute of Science Education and the Division of Science Education, Chonbuk National University, Jeonju 561-756, Korea*

Sung Jin An, Jinkyong Yoo, and Gyu-Chul Yi

*National CRI Center for Semiconductor Nanorods and the Department of Materials Science and Engineering, Pohang University of Science and Technology (POSTECH), Pohang 790-784, Korea*

(Received 20 November 2005; accepted 14 February 2006; published online 16 March 2006)

The structure of tubular GaN coaxially grown on ZnO nanorods with thickness of 6–12 nm was investigated using x-ray absorption fine structure (XAFS) at the Ga *K* edge. The XAFS measurements revealed that the GaN had a distorted-wurtzite structure, and that there were more distortions in the bond length of Ga–Ga pairs than in Ga–N pairs. However, no extra disorders were observed in any of the pairs. These results strongly suggest that Ga atoms first bonded to the ZnO template. Unlike other techniques, the XAFS determines structure around a selected species atom in nano-heterostructures. © 2006 American Institute of Physics. [DOI: 10.1063/1.2185627]

It is known that in nanoparticles, structural properties as well as particle size play an important role in the determination of physical and electrical properties.<sup>1–3</sup> Therefore, it is definitely necessary to know the structural properties for better understanding of the nano-materials. Diffraction is a canonical tool to measure crystalline structure, however, it is limited in terms of investigating nano materials which consist of just a small number of atoms. It is particularly difficult to determine the structural properties of the nano-heterostructures which have been intensively studied for practical applications, light emitting diodes,<sup>4</sup> for example. Transmission electron microscopy (TEM) can detect local structural properties. However, the TEM measurements require destruction of the specimens. Moreover, TEM cannot distinguish atomic species. In this letter, we demonstrate that x-ray absorption fine structure (XAFS) has a great capability to determine the local structure around a specific species atom in nano-heterostructures. We have chosen GaN/ZnO coaxial nanorod heterostructures especially for the XAFS study because GaN and ZnO have similar lattice constants and other techniques cannot precisely determine the structural properties of the heterostructure.

Since the fabrication of GaN nanotubes, after casting on ZnO nanorods,<sup>5</sup> nanotubular GaN structures have been studied widely for their potential applications as well as for fundamental research. Ultrafine GaN nanotubes have been fabricated by capping GaN on various templates, such as ZnO nanorods,<sup>5,6</sup> GaP<sup>7</sup> and others. X-ray diffraction (XRD) measurements from tubular GaN nanocrystals in GaN/ZnO heterostructures have suggested that it might be a wurtzite (WZ, *P6<sub>3</sub>mc*) structure.<sup>5,6</sup> However, it was not conclusive because the XRD could detect only averaged crystalline structure. Moreover, it could not clearly distinguish the GaN capping layer from the ZnO template due to similar lattice constants. To clarify the orientation-dependent structural properties of the GaN/ZnO heterostructures, we employed orientation-dependent XAFS which can describe the angles and distances of neighboring atoms from a probe atom.<sup>8</sup> Two inde-

pendent XAFS measurements from the vertically aligned GaN/ZnO coaxial nanorods were made with the x-ray polarizations parallel and perpendicular to the nanorod length direction. Both sets of XAFS data were *simultaneously* fitted with the same parameters and the orientation-dependent structural properties of the tubular GaN crystals were obtained and compared with their bulk counterparts.

Ultrafine GaN/ZnO coaxial heterostructures were synthesized using catalyst-free metal-organic vapor-phase epitaxy (MOVPE). Vertically well-aligned ZnO nanorods with an average diameter and length of about 50 nm and 1  $\mu\text{m}$ , respectively, were grown on Si [001] substrates at about 500 °C, and subsequently, an ultrafine GaN capping layer was deposited on the pre-grown ZnO nanorods *in situ* with MOVPE.<sup>6</sup> To study the structural strain effect on the structural distortion of the GaN layer due to the lattice mismatch between the ZnO template and GaN layer, we prepared two specimens with an average GaN layer thickness of  $6 \pm 1$  and  $12 \pm 1$  nm. High-resolution synchrotron XRD and high-resolution transmission electron microscopy (TEM) revealed that the ZnO nanorods were well-ordered single crystals, and the capping GaN layer covered the ZnO nanorods uniformly.<sup>6</sup> We also prepared GaN powder with a purity of 99.99% and the particle size of less than 25  $\mu\text{m}$  as a counterpart for comparison with the structural properties of the tubular GaN nanocrystals. At 20 K, XAFS measurements with transmission and fluorescence modes for the GaN powder and GaN/ZnO coaxial nanorods, respectively, at the Ga *K* edges (10 367 eV) were performed by selecting the incident x-ray energy with a 25% detuned Si(111) double monochromator at the PNC-CAT of the Advanced Photon Source, Argonne National Laboratory.

Figure 1 shows the normalized total x-ray absorption and x-ray absorption coefficients from GaN powder and GaN/ZnO coaxial nanorods, respectively. For the GaN/ZnO coaxial nanorods, the fluorescence XAFS data were collected with the two orientations, parallel and perpendicular to the nanorod length direction. Polarization efficiency of 95% was taken into account in the data analysis. The x-ray self-absorption of the GaN nanotubes with about 1  $\mu\text{m}$  length at Ga *K* edge was negligible. The x-ray absorption near edge

<sup>a)</sup> Author to whom correspondence should be addressed; electronic mail: swhan@chonbuk.ac.kr.

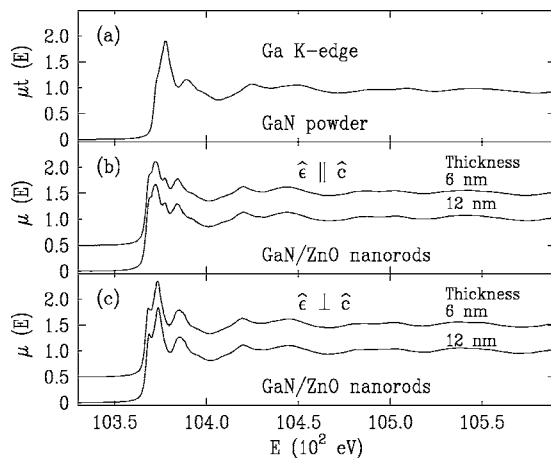


FIG. 1. Normalized x-ray absorption coefficient from (a) GaN powder and (b),(c) GaN/ZnO coaxial heterostructures as a function of incident x-ray energy at the Ga *K* edge and 20 K. For the GaN/ZnO coaxial structures, the XAFS data were collected with the geometry of the *ĉ* axis aligned, (b) parallel and (c) perpendicular, to the electric field vector ( $\hat{\epsilon}$ ) of the incident x rays.

structure from the GaN nanotubes clearly demonstrates orientation dependence. This is comparable to the ZnO nanorods with a wurtzite structure.<sup>2</sup> The local structures around the Ga atoms can be obtained by looking at the fine structure above the absorption edge. The XAFS data were analyzed with the UWXAFS package<sup>9</sup> using standard procedures.<sup>8</sup> The orientation-dependent XAFS data from the tubular GaN crystals are presented in Fig. 2. To minimize uncertainties only the XAFS data in the *k* range of 3.0–12.5 Å<sup>-1</sup> were used for further analysis. The dotted lines in Fig. 3 show the magnitudes of the Fourier transformed XAFS data from the GaN powder and GaN/ZnO heterostructures. It should be noted that the peaks shifted by about 0.4 Å on the  $\tilde{r}$  axis from their true bond lengths due to the phase shift of the backscattered photoelectrons. Detailed fits are therefore necessary to obtain quantitative information.

The XAFS data Fourier transformed to *r* space were fitted to the theoretical XAFS calculations,<sup>10</sup> as shown in Fig. 3. The fits included single- and multi-scattering paths. The GaN powder data was fitted with a fully occupied model of a wurtzite (WZ) structure, as shown in Fig. 3(a). We also fit the data with a cubic zinc blende (ZB,  $F\bar{4}3m$ ) structure and obtained a reasonably good fit (not shown here). However, in the fit the values of *r*-factor and  $\chi^2_\nu$  which were defined elsewhere<sup>8</sup> with the ZB model were about three times greater

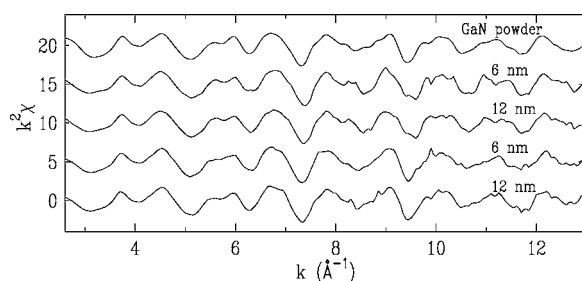


FIG. 2. XAFS ( $k^2\chi$ ) from GaN powder (top) and from the aligned GaN/ZnO coaxial structures with thickness of 6 and 12 nm for  $\hat{\epsilon} \parallel \hat{c}$  (2nd and 3rd) and  $\hat{\epsilon} \perp \hat{c}$  (4th and 5th), as a function of the photoelectron wave vector,  $k = \sqrt{2m(E - E_0)}/\hbar$ , where *m* is the electron rest mass, *E* is the incident photon energy and  $E_0$  is the edge energy.

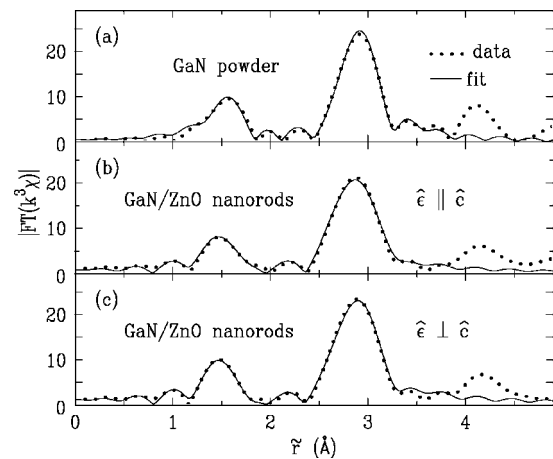


FIG. 3. Magnitude of Fourier transformed XAFS, from (a) GaN powder and GaN/ZnO coaxial structures with an average GaN thickness of 6 nm for (b)  $\hat{\epsilon} \parallel \hat{c}$  and (c)  $\hat{\epsilon} \perp \hat{c}$ , as a function of the distance from a Ga atom. For the Fourier transformation, a Hanning window with a window sill width of 0.5 Å<sup>-1</sup> was used. Data in the range of  $\tilde{r} = 1.2 - 3.3$  Å were fitted.

than those with the WZ structure. The fits imply that the GaN powder had a WZ structure. Both the ZB and WZ structures have a similar tetrahedral environment that Ga(N) has four N(Ga) and 12 Ga(N) atoms as the first and second neighboring atoms. For GaN with a ZB structure, the bond lengths of the four Ga–N and 12 Ga–Ga pairs are  $\sim 1.93$  and 3.15 Å, respectively. However, in an ideal WZ phase, the Ga–N and Ga–Ga pairs have slightly different bond lengths: the bond length of one Ga–N(1) pairs located just below Ga along the *c* axis is slightly larger than those of the three other Ga–N(2) pairs located at  $\sim 20^\circ$  off from the *ab* plane, and six Ga–Ga(1) pairs located about  $55^\circ$  off from the *ab* plane also have a longer bond length than the other six Ga–Ga(2) pairs located in the *ab* plane. Therefore, the structural space group can be determined with the bond lengths of the Ga–N and Ga–Ga pairs which correspond to the first and second peaks in Fig. 3. The fit to the XAFS data of the GaN powder revealed that both the bond lengths of the Ga–N(1) and Ga–Ga(1) pairs are about 0.025 Å bigger than those of Ga–N(2) and Ga–Ga(2) pairs. These results roughly agreed with a previous XRD study.<sup>11</sup> The fit results are summarized in Table I. The two sets of XAFS data measured at the electric field of the incident x-ray parallel and perpendicular to the *c* axis can independently determine the bond lengths and their disorders of Ga–N(1), Ga–N(2), Ga–Ga(1) and Ga–Ga(2) pairs.

The two sets of data shown in Figs. 3(b) and 3(c) were simultaneously fitted to the XAFS theoretical calculation,<sup>10</sup> varying the bond lengths, Debye–Waller factors ( $\sigma^2$ , including thermal vibration and static disorder) and coordination numbers. Although the fit started with a WZ structure, both the WZ and ZB structures were reflected because the bond lengths of the Ga–N(1), Ga–N(2), Ga–Ga(1) and Ga–Ga(2) pairs were independently varied in the fit. The results of the best fit are presented in Table I. The fits revealed that the bond length of the Ga–N(1) in the GaN nanocrystals with a thickness of 12 nm was larger by 0.02 Å than that of the Ga–N(2) pairs. As the GaN thickness was reduced to 6 nm, the Ga–N(2) and Ga–N(1) pairs had a similar bond length with about 0.01 Å distortion, in comparison with the bulk counterpart. These results strongly suggest that the GaN capping layer has a ZB structure in the beginning of GaN

TABLE I. Coordination number ( $N$ ), bond length ( $d$ ) and Debye–Waller factor ( $\sigma^2$ ) of powder and tubular GaN were obtained with XAFS at 20 K.  $S_0^2$  of 0.85(5) were determined from the fit to the GaN powder data and fixed in the tubular data fits. For the model calculations, the WZ structure with  $a=b=3.160$  Å,  $c=5.195$  Å and the crystalline symmetry  $z$  of nitrogen = 0.375 were used. For the ZB structure, the lattice constant of 4.52 Å was used.

WZ structure	$N$	Ga–N(1)		$N$	Ga–N(2)		$N$	Ga–Ga(1)		$N$	Ga–Ga(2)	
		$d$ (Å)	$\sigma^2$ (Å <sup>2</sup> )		$d$ (Å)	$\sigma^2$ (Å <sup>2</sup> )		$d$ (Å)	$\sigma^2$ (Å <sup>2</sup> )		$d$ (Å)	$\sigma^2$ (Å <sup>2</sup> )
Model	1	1.94813		3	1.93632		6	3.17420		6	3.16000	
GaN powder	1	1.947(5)	0.0032(5)	3	1.920(5)	0.0032(5)	6	3.206(6)	0.0050(6)	6	3.179(6)	0.0050(6)
GaN/ZnO (12 nm)	1.1(1)	1.942(5)	0.0039(7)	3.2(3)	1.918(4)	0.0036(7)	6.0(2)	3.195(3)	0.0049(3)	6.0(2)	3.195(3)	0.0048(3)
GaN/ZnO (6 nm)	1.1(1)	1.940(3)	0.0041(3)	3.3(3)	1.930(3)	0.0024(3)	6.1(4)	3.195(4)	0.0043(2)	6.2(4)	3.195(3)	0.0053(2)

ZB structure	$N$	Ga–N		$N$	Ga–Ga	
		$d$ (Å)	$\sigma^2$ (Å <sup>2</sup> )		$d$ (Å)	$\sigma^2$ (Å <sup>2</sup> )
Model	4	1.95722		12	3.19612	
Powder	4	1.954(6)	0.0036(10)	12	3.193(6)	0.0051(3)

growth, due to the structural strain from the lattice mismatch between the GaN and ZnO. For an ideal WZ structure of GaN, the bond length of Ga–Ga(1) pairs was about 0.03 Å shorter than that of Ga–Ga(2) pairs. However, the XAFS revealed that the Ga–Ga pairs have the same bond length 3.195 Å, independent of the directions. It should be emphasized that the bond lengths of Ga–Ga(1) and Ga–Ga(2) pairs were independently determined from the fit of the second peaks in Figs. 3(b) and 3(c), respectively. Based on the bond lengths, we concluded that the GaN capping layers have a distorted-WZ structure or a ZB-like structure. Our observations correspond with a previous TEM study which showed a structural distortion near the interface of the GaN/ZnO coaxial nanorods.<sup>6</sup>

The bond length of Ga–N pairs, 1.935 Å, in the GaN nanotubes was very similar to that in the bulk counterpart. However, it was somewhat different from the theoretical works that predicted 1.78 Å<sup>7</sup> and 1.88 Å,<sup>12</sup> assuming GaN nanotubes formed into a graphitic sheet. The Ga–Ga pairs in the nanocrystals have a bond length of 3.2 Å which is ~0.07 Å shorter than that in the bulk counterpart. This is very comparable to the Zn–Zn bond length of 3.22 Å in the ZnO nanorod templates.<sup>2</sup> A previous study revealed that the terminating atoms at the lateral surface of the ZnO nanorods were oxygen.<sup>2</sup> During the GaN growth, the gallium atoms might first be deposited on the oxygen-rich surface instead of the nitrogen atoms. Subsequently, nitrogen atoms were deposited on the Ga layer. After that, gallium and nitrogen layers were deposited repeatedly. In this case, the bond length of Ga–Ga pairs was more greatly affected by the ZnO template.

The  $\sigma^2$ s of the Ga–N and Ga–Ga pairs, except the Ga–N(1) pairs in the GaN nanocrystals showed no extra disorders compared to those in the bulk counterpart, as shown in Table I. The tubular GaN crystals can be formed by a GaN slab that was observed in carbon nanotubes,<sup>13</sup> or depositions of gallium and nitrogen layers by turns. In the first case, one can expect more disorders/distortion in the perpendicular direction ( $ab$  plane) than along the tube length direction ( $c$  axis) because the bonds in the  $ab$  plane are less tight and more distorted due to bending than those along the  $c$  axis. The  $\sigma^2$ s suggested neither extra disorders nor distortion existing in the bonds in the  $ab$  plane of the GaN nanotubes, compared with the bulk GaN counterpart. This provides more evidence that Ga atoms first bonded together on oxygen in the surface of the ZnO template and, subsequently,

Ga and N atoms formed into a single solid, tubular crystal. This result also implies that interdiffusion at the GaN/ZnO interface is negligible, and that the tubular GaN electrically contact the ZnO template well. Our observations correlated well with a previous TEM study<sup>6</sup> and the theoretical work by Xu who showed that a tubular GaN single crystal with [100]-orientation lateral facet more stable than with [110] orientation.<sup>14</sup>

In conclusion, the structural environments around Ga in GaN tubes coaxially grown on ZnO nanorod templates were studied by the orientation-dependent XAFS. The XAFS measurements revealed that the GaN crystals in the GaN/ZnO heterostructures had a ZB structure in the beginning of growth, and became a WZ structure, as the tubes thickened. We observed that Ga atoms were first deposited on the surface of the ZnO template, so that Ga–Ga bond length was more distorted than Ga–N pairs.

Work at Chonbuk National University was conducted under the auspices of the Korean MOST through PEPF User Program as a part of the 21C Frontier R&D Program and the Korean MOCIE through the New Technology R&D Program. Work at POSTECH was supported by the National Creative Research Initiative Project of the MOST. The PNC-CAT beamline was supported by the U.S. DOE.

<sup>1</sup>W. P. Halperin, Rev. Mod. Phys. **58**, 533 (1986).

<sup>2</sup>S.-W. Han, H.-J. Yoo, S.-J. An, J. Yoo, and G.-C. Yi, Appl. Phys. Lett. **86**, 21917 (2005).

<sup>3</sup>W. I. Park, Y. H. Jun, S. W. Jung, and G.-C. Yi, Appl. Phys. Lett. **82**, 964 (2003); W. I. Park, G.-C. Yi, M. Kim, and S. J. Pennycook, Adv. Mater. (Weinheim, Ger.) **14**, 1841 (2002).

<sup>4</sup>R. Konenkamp, R. C. Word, and M. Godinez, Nano Lett. **5**, 2005 (2005).

<sup>5</sup>J. Goldberger, R. He, Y. Zhang, S. Lee, H. Yan, H.-J. Choi, and P. Yang, Nature (London) **422**, 599 (2003).

<sup>6</sup>S. J. An, W. I. Park, G.-C. Yi, Y.-J. Kim, and H.-B. Kang, Appl. Phys. Lett. **84**, 3612 (2004).

<sup>7</sup>M. W. Lee, H. C. Hsueh, H.-M. Lin, and C.-C. Chen, Phys. Rev. B **67**, 161309 (2003).

<sup>8</sup>S.-W. Han, E. A. Stern, D. Hankel, and A. R. Moodenbaugh, Phys. Rev. B **66**, 94101 (2002).

<sup>9</sup>E. A. Stern, M. Neville, B. Ravel, Y. Yacoby, and D. Haskel, Physica B **208**, 209, 117 (1995).

<sup>10</sup>A. L. Ankudinov, B. Ravel, J. J. Rehr, and S. D. Conradson, Phys. Rev. B **58**, 7565 (1998).

<sup>11</sup>C. Roder, S. Einfeldt, S. Figge, and D. Hommel, Phys. Rev. B **72**, 85218 (2005).

<sup>12</sup>S. Hao, G. Zhou, J. Wu, W. Duan, and B.-L. Gu, Phys. Rev. B **69**, 113403 (2004).

<sup>13</sup>S. Iijima, Nature (London) **354**, 56 (1991).

<sup>14</sup>B. Xu, A. J. Lu, B. C. Pan, and Q. X. Yu, Phys. Rev. B **71**, 125434 (2005).